nature COMMUNICATIONS

ARTICLE

Received 24 Sep 2014 | Accepted 28 Jan 2015 | Published 4 Mar 2015

DOI: 10.1038/ncomms7433

Controlling superconductivity by tunable quantum critical points

S. Seo[1], E. Park[1], E.D. Bauer[2], F. Ronning[2], J.N. Kim[3], J.-H. Shim[3], J.D. Thompson[2] & Tuson Park[1]

The heavy fermion compound $CeRhIn_5$ is a rare example where a quantum critical point, hidden by a dome of superconductivity, has been explicitly revealed and found to have a local nature. The lack of additional examples of local types of quantum critical points associated with superconductivity, however, has made it difficult to unravel the role of quantum fluctuations in forming Cooper pairs. Here, we show the precise control of superconductivity by tunable quantum critical points in $CeRhIn_5$. Slight tin-substitution for indium in $CeRhIn_5$ shifts its antiferromagnetic quantum critical point from 2.3 GPa to 1.3 GPa and induces a residual impurity scattering 300 times larger than that of pure $CeRhIn_5$, which should be sufficient to preclude superconductivity. Nevertheless, superconductivity occurs at the quantum critical point of the tin-doped metal. These results underline that fluctuations from the antiferromagnetic quantum criticality promote unconventional superconductivity in $CeRhIn_5$.

[1] Department of Physics, Sungkyunkwan University, Suwon 440-746, South Korea. [2] Condensed Matter and Magnet Science, Los Alamos National Laboratory, Los Alamos, New Mexico 87545, USA. [3] Department of Chemistry, Pohang University of Science and Technology, Pohang 790-784, South Korea. Correspondence and requests for materials should be addressed to J.D.T. (email: jdt@lanl.gov) or to T.P. (email: tp8701@skku.edu).

Strange metallic behaviour arises from incoherent electron scattering by critical fluctuations that emerge from a continuous quantum phase transition at absolute zero temperature[1,2]. Unconventional superconductivity is a potential ordered quantum state that subsumes entropy generated by the proliferation of fluctuations emanating from the quantum critical point (QCP)[3–5]. In this case, the spectrum of associated quantum fluctuations determines the structure of the superconducting (SC) gap[6–9]. Although several classes of unconventional superconductors have been discovered in proximity to a $T=0$ magnetic instability, the role that associated fluctuations play in forming SC Cooper pairs is still debatable. Often a projected QCP is hidden by superconductivity, but $CeRhIn_5$ is a rare example where the hidden QCP has been revealed by an applied magnetic field, exposing strange metallic behaviour and emphasizing the close interplay between quantum criticality and superconductivity[4]. However, scarcity of additional examples of a revealed QCP that otherwise is hidden under a SC dome raises the questions of whether unconventional superconductivity is indeed a manifestation of an ordered phase arising from quantum fluctuations and whether that superconductivity can be controlled by a tunable QCP.

At atmospheric pressure, the heavy fermion metal $CeRhIn_5$ orders antiferromagnetically below 3.8 K ($=T_N$), where spins of Ce 4*f* electrons are anti-aligned within the Ce-In plane and rotate incommensurately by 106.9° in the adjacent plane along the tetragonal *c* axis[10,11]. Applied pressure *P* suppresses T_N and induces superconductivity that coexists microscopically with magnetic order up to a critical pressure of 1.75 GPa where, in the absence of an applied magnetic field, Néel order abruptly disappears and is replaced by superconductivity. The dome of pressure-dependent superconductivity $T_c(P)$ is a maximum at 2.3 GPa, the pressure where the antiferromagnetic (AFM) QCP is revealed by an applied magnetic field[4]. T_N of $CeRhIn_5$ also is suppressed gradually with Sn substitution for In and reaches 0 K at a critical concentration $x_c=0.07$, $CeRh(In_{1-x}Sn_x)_5$ (refs 12,13). A gradual enhancement of the electronic Sommerfeld coefficient of specific heat with decreasing temperature and a sub-*T* linear dependence of the electrical resistivity at x_c are consistent with the non-Fermi-liquid behaviours that are observed at the pressure- and field-induced QCP of pure $CeRhIn_5$, but with less singularity possibly due to effects of disorder from Sn substitution that also prevent the development of superconductivity at x_c. The variation of T_N with Sn concentration suggests that the position of a pressure-induced QCP in a sample with $x<x_c$ may be shifted to a lower pressure relative to pristine $CeRhIn_5$ because Sn doping enhances hybridization between the local Ce 4*f* spin and itinerant electrons (as shown in Supplementary Fig. 1 and Supplementary Note 1), therefore acting as effective positive pressure. If the unconventional superconductivity of $CeRhIn_5$ was to arise from an attractive pair interaction mediated by quantum critical fluctuations, pressure-induced superconductivity in lightly Sn-doped $CeRhIn_5$ would be expected to be controlled by its QCP.

In the following, we present electrical resistivity measurements of 4.4% Sn-doped $CeRhIn_5$ under pressure and magnetic field, which reveals that Sn doping shifts the AFM QCP from 2.3 GPa to 1.3 GPa in undoped $CeRhIn_5$. This slight Sn substitution leads to a residual impurity scattering that is 300 times larger at atmospheric pressure than that of pure $CeRhIn_5$, which should preclude the possibility of superconductivity. In spite of this strong scattering, pressure-induced superconductivity in the Sn-doped metal emerges and reaches a maximum T_c at the QCP of 1.3 GPa. Above T_c, the temperature exponent of resistivity is sub-linear, manifesting strange metallic behaviour emanating from the absolute zero temperature instability. Taken together with the precise control of superconductivity by doping- and pressure-tuned QCPs, these results show that it is the QCP that controls the appearance of the unconventional SC phase.

Results

Electrical resistivity and anomalous electron scattering. The colour contour map in Fig. 1a describes the evolution of absolute values of the *c* axis electrical resistivity (ρ_c) of 4.4% Sn-doped $CeRhIn_5$ at 5 Tesla, a field slightly higher than the SC upper critical field over the whole pressure range studied. Strong enhancement of ρ_c is centred around 1.3 GPa, showing a funnel-shape topology. Isothermal resistivity at the base temperature of 0.3 K also is enhanced near 1.3 GPa, being a factor of 1.7 times larger than that at 2.46 GPa (see Supplementary Fig. 2 and Supplementary Note 2). In the absence of a magnetic field, as shown in Fig. 1b, a pressure-induced SC phase as well as magnetic order appear. In this limit, T_N gradually decreases with pressure and disappears when it becomes smaller than T_c; whereas, $T_c(P)$ is dome shaped with maximal T_c at 1.3 GPa (phase transitions in resistivity are shown in Supplementary Fig. 3b for representative

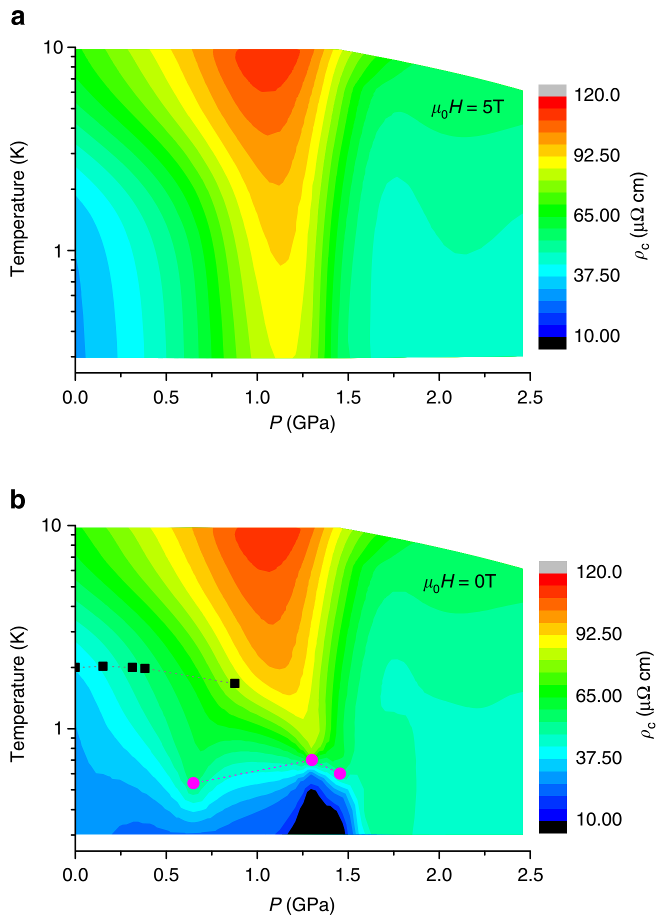

Figure 1 | Electrical resistivity of 4.4% Sn-doped $CeRhIn_5$ under pressure. (**a**) A contour map of the *c* axis electrical resistivity (ρ_c) is plotted in the pressure–temperature plane for a magnetic field of 5 Tesla, which is slightly larger than $\mu_0H_{c2}(0)$. The colours represent absolute values of ρ_c, where a funnel of enhanced electronic scattering emerges near 1.3 GPa. (**b**) Contour map of ρ_c is plotted for a magnetic field of 0 Tesla. The antiferromagnetic transition and superconducting transition temperatures are plotted in square and circle symbols, respectively. T_c is assigned as the onset point of the phase transition. Data representative of those from which this map was constructed are shown in Supplementary Fig. 3.

pressures). Although the contour of ρ_c is influenced by the presence of new broken symmetries at low temperatures, it shows a similar enhancement of ρ_c above T_c at the optimal pressure (P_c). Complete suppression of T_N near P_c provides compelling evidence that the anomalous enhancement of ρ_c in the pressure–temperature plane is a consequence of critical fluctuations from an AFM QCP under the SC dome of Sn-doped $CeRhIn_5$.

QCP and sub-*T* linear resistivity. The local temperature exponent n of ρ_c at 5 Tesla, where $n = \partial \ln \Delta\rho / \partial \ln T$ and $\Delta\rho = \rho_c - \rho_0 = AT^n$, also is anomalous near 1.3 GPa, as shown in Fig. 2a. The residual resistivity ρ_0 reflects impurity scattering that depends on both the amount of disorder and the effective impurity potential, which itself is enhanced by critical fluctuations[14]. The colour contour that describes the local exponent n reveals a sub-linear temperature dependence in a narrow pressure–temperature plane around 1.3 GPa and low temperatures, a hallmark of quantum critical behaviour, and the resistivity follows a Fermi-liquid T^2 dependence elsewhere. Figure 2b–d representatively show the low temperature $\rho_c(T)$ at 5 Tesla for pressures of 100 kPa ($<P_c$), 1.3 GPa ($=P_c$) and 1.92 GPa ($>P_c$) in the top, middle and bottom panels, respectively. At ambient pressure, a Landau–Fermi T^2 dependence is observed below 2.3 K and the residual resistivity is 30.2 $\mu\Omega$ cm, which is about 300 times larger than that of pure $CeRhIn_5$ ($=0.1$ $\mu\Omega$ cm) due to potential scattering by impurities. The T^2 coefficient A is 1.98 $\mu\Omega \, cm \, K^{-2}$, which corresponds to a Sommerfeld-specific heat coefficient $\gamma = 445$ mJ mol^{-1} K^{-2} from the Kadowaki–Woods relation[15], confirming that Sn-doped $CeRhIn_5$ is a heavy electron system. At 1.38 GPa, the pressure where T_c is a maximum at zero magnetic field, $\rho_c(T)$ deviates from a T^2 dependence, following a sub-T linear dependence over an extended temperature range from the base temperature ($=0.3$ K) to 7 K, that is, $\rho_c = \rho_0 + AT^n$ with $n = 0.69$ and $\rho_0 = 78.5$ $\mu\Omega$ cm. We note that the fitting parameters are $n = 0.71$ and $\rho_0 = 5.2$ $\mu\Omega$ cm for pure $CeRhIn_5$ at 2.35 GPa, the QCP, as well as the optimal pressure for superconductivity[16].

The residual resistivity ρ_0 is much larger in Sn-doped $CeRhIn_5$ than in pure $CeRhIn_5$ at their respective critical pressures, but the exponent n at the QCP is independent of disorder, indicating that the inelastic scattering that governs the temperature dependence is of the same origin and is from quantum critical fluctuations. A sub-linear temperature dependence is not anticipated in conventional models of criticality that only consider electron scattering from critical fluctuations of magnetization[4]. On the other hand, a similar sub-T linear behaviour in ρ has been reported in the unusual quantum critical metal $YbRh_2Si_2$ (ref. 17), whose$T^{3/4}$ resistivity is interpreted in the context of a critical quasiparticle theory that includes the interaction of heavy quasiparticles with three-dimensional AFM fluctuations in the non-Gaussian critical region[18]. In this context for Sn-doped $CeRhIn_5$, $\rho_c(T)$ should recover a normal metallic temperature-squared dependence at pressures higher than P_c, which it does. As illustrated in Fig. 2d, ρ_0 decreases to 47.2 $\mu\Omega$ cm and A is 0.56 $\mu\Omega \, cm \, K^{-2}$, which corresponds to a Sommerfeld coefficient of 236 mJ mol^{-1} K^{-2}. The anomalous temperature dependence of the resistivity and strong enhancement of ρ_0 and A at P_c imply that the putative QCP lies at P_c, the pressure where $T_c(P)$ is highest (see Fig. 3b and Supplementary Note 3).

Discussion

Global temperature–pressure phase diagrams of pure $CeRhIn_5$ and 4.4% Sn-doped $CeRhIn_5$ are plotted in Fig. 3a. The similarity in the pressure dependence of the magnetic and SC phases of both compounds is apparent, although T_N differs almost by a factor of two: (1) A pressure-induced dome of superconductivity exists in both systems, but the maximum T_c is shifted from 2.3 GPa for the undoped to 1.3 GPa for the 4.4% Sn-doped $CeRhIn_5$. (2) T_N initially increases with increasing pressure, decreases with further pressure and abruptly disappears when the pressure-induced T_c exceeds T_N, suggesting that long-range AFM

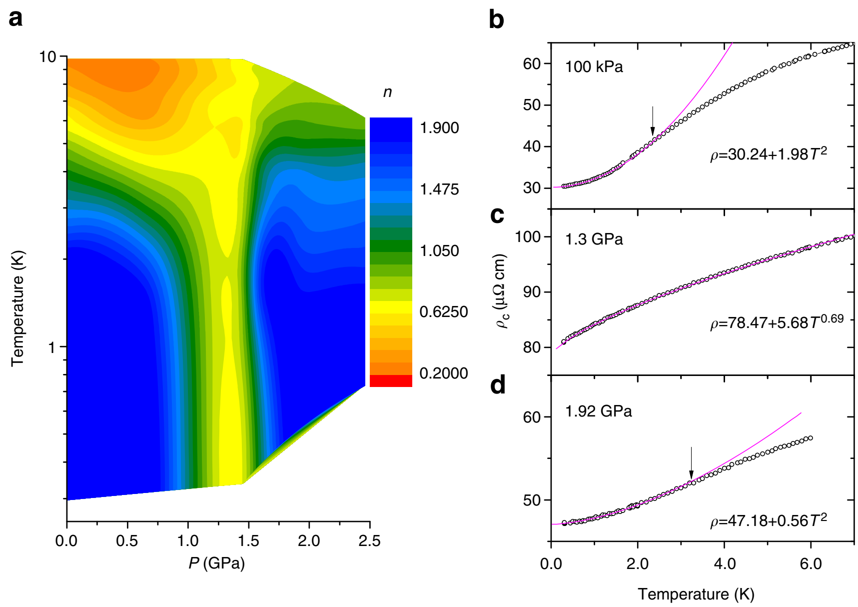

Figure 2 | Non-Fermi-liquid electrical resistivity (ρ_c) of 4.4% Sn-doped $CeRhIn_5$ under pressure. (**a**) Colours represent the local exponent, $n = \partial \ln \Delta\rho / \partial \ln T$, at 5 Tesla, where $\Delta\rho = \rho_c - \rho(T = 0\,K) = AT^n$. The resistivity ρ_c was measured along the crystalline c axis. The sub-T linear dependence of ρ_c at 1.3 GPa is a hallmark of unconventional non-Fermi liquids. (**b**) Low temperature resistivity ρ_c is plotted at pressures of 0.001, 1.3 and 1.92 GPa in (**b**), (**c**) and (**d**), respectively. The solid lines are least-squares fits of $\rho_c = \rho(T = 0\,K) + AT^n$. The resistivity deviates from Landau–Fermi T^2 behaviour at the QCP ($=1.3$ GPa), but it follows a T^2 dependence at pressures away from the QCP. Arrows mark the Fermi liquid temperature T_{FL} below which $\rho_c \propto T^2$ and other pressures results are shown in Supplementary Fig. 4.

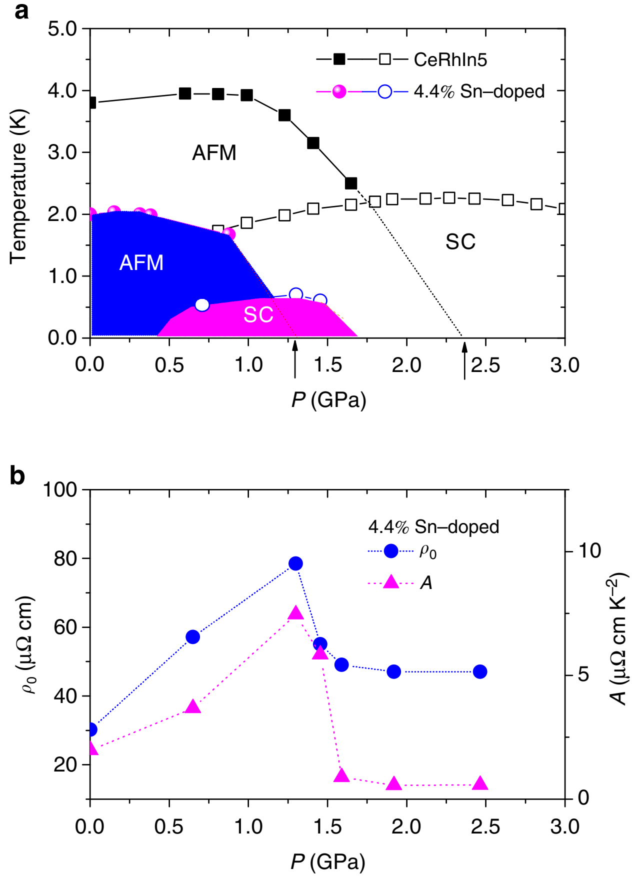

Figure 3 | Pinning of T_c maximum via a QCP. (**a**) Resistively determined pressure–temperature phase diagrams are plotted at zero magnetic field for $CeRhIn_5$ (squares) and 4.4% Sn-doped $CeRhIn_5$ (circles). Solid symbols denote the antiferromagnetic (AFM) transition temperature (T_N) and open symbols describe the superconducting transition temperature (T_c). The maximum T_c is lower in Sn-doped $CeRhIn_5$ because of pair-breaking arising from strong impurity scattering. Arrows on the x axis indicate the AFM QCPs at 1.3 GPa for 4.4% Sn-doped and at 2.3 GPa for pure $CeRhIn_5$, respectively. (**b**) Pressure dependence of the residual resistivity ρ_0 (circles) and T^2 coefficient A (triangles) of ρ_c for 4.4% Sn-doped $CeRhIn_5$ are plotted on the left and right ordinates, respectively. These parameters were obtained by a least-squares fit of the c axis electrical resistivity at 5 Tesla by using $\rho_c = \rho_0 + AT^2$ (see Supplementary Note 4).

order arises from RKKY (Ruderman–Kittel–Kasuya–Yosida) interactions (see Supplementary Fig. 3). (3) A T_c maximum occurs at the QCP for both compounds, confirming that critical quantum fluctuations are the source of unconventional superconductivity. (4) The dependence on temperature of ρ_c at the QCP is sub-linear in the normal state, which reflects the unconventional nature of the QCP.

Although there are many cases of superconductors near spin-density-wave QCPs[19–24], superconductivity in a metal whose quantum criticality is unconventional[4], for example, $YbRh_2Si_2$, $CeCu_{6-x}Au_x$ and $CeRhIn_5$ has been rare, raising a question whether the associated critical bosonic and fermionic fluctuations can provide the necessary attractive interaction to form Cooper pairs. Clear identification of the QCP in 4.4% Sn-doped $CeRhIn_5$ and its sub-T linear temperature dependence of ρ_c in the normal state indicate that unconventional superconductivity is promoted by an unconventional QCP. Recent numerical calculations have found that singlet-pairing correlations are enhanced at such a QCP[25]. Nucleation of unconventional superconductivity at the respective QCPs of Sn-doped and pristine $CeRhIn_5$ attests that superconductivity is pinned to the QCPs because the associated critical fluctuations are the source of the pairing glue. These results provide a way to control unconventional superconductivity and motivate theoretical and experimental imperatives to elucidate the mechanism of QCP-induced superconductivity, especially in metals whose criticality involves both bosonic and fermionic degrees of freedom.

Methods

Crystal synthesis and experiments in pressure. Single crystals of $CeRh(In_{1-x}Sn_x)_5$ were synthesized by a standard In-flux technique. Basic physical properties of $CeRh(In_{1-x}Sn_x)_5$ were measured previously[12]. The c axis electrical resistivity measurements were performed under pressure for samples with a Sn concentration $x = 0.044$, where the value of x was determined by microprobe analysis. Pressure work was performed using a hybrid Be–Cu/NiCrAl clamp-type pressure cell with silicone fluid as the pressure medium to ensure hydrostatic condition for pressure up to 2.5 GPa. Pressure in the cell was determined from the pressure-dependent SC transition temperature of a Pb manometer using the pressure scale of Eiling and Schilling[26]. A standard four-probe configuration, using spot-welded contacts, was used to measure the c axis electrical resistivity with an LR700 Resistance Bridge. Two different cryostats were used to control temperature and magnetic field: a ^4He cryostat for temperature measurements from 300 to 1.2 K and a ^3He cryostat for temperatures from 10 down to 0.3 K and for magnetic fields up to 5 Tesla.

References

1. Lohneysen, H. v., Rosch, A., Vojta, M. & Wolfle, P. Fermi-liquid instabilities at magnetic quantum phase transitions. *Rev. Mod. Phys.* **79,** 1015–1075 (2007).
2. Stewart, G. R. Non-Fermi-liquid behavior in d- and f-electron metals. *Rev. Mod. Phys.* **73,** 797–855 (2001).
3. Keimer, B., Kivelson, S. A., Norman, M. R., Uchida, S. & Zaanen, J. From quantum matter to high-temperature superconductivity in copper oxides. *Nature.* **518,** 179–186 (2015).
4. Park, T. *et al.* Hidden magnetism and quantum criticality in the heavy fermion superconductor $CeRhIn_5$. *Nature* **440,** 65–68 (2006).
5. Knebel, G., Aoki, D., Braithwaite, D., Salce, B. & Flouquet, J. Coexistence of antiferromagnetism and superconductivity in $CeRhIn_5$ under high pressure and magnetic field. *Phys. Rev. B* **74,** 020501(R) (2006).
6. Mathur, N. D. *et al.* Magnetically mediated superconductivity in heavy fermion compounds. *Nature* **394,** 39–43 (1998).
7. Coleman, P. & Schofield, A. J. Quantum criticality. *Nature* **433,** 226–229 (2005).
8. Monthoux, P., Pines, D. & Lonzarich, G. G. Superconductivity without phonons. *Nature* **450,** 1177–1183 (2007).
9. Watanabe, S., Imada, M. & Miyake, K. Superconductivity emerging near quantum critical point of valence transition. *J. Phys. Soc. Jpn* **75,** 043710 (2006).
10. Hegger, H. *et al.* Pressure-induced superconductivity in quasi-2D $CeRhIn_5$. *Phys. Rev. Lett.* **84,** 4986–4989 (2000).
11. Bao, W. *et al.* Incommensurate magnetic structure of $CeRhIn_5$. *Phys. Rev. B* **62,** R14621 (2000).
12. Bauer, E. D. *et al.* Antiferromagnetic quantum critical point in $CeRhIn_{5-x}Sn_x$. *Physica B* **378–380,** 142–143 (2006).
13. Knebel, G. *et al.* Antiferromagnetism and superconductivity in $CeRhIn_5$. *J. Phys. Soc. Jpn* **80,** SA001 (2011).
14. Miyake, K. & Narikiyo, O. Enhanced impurity scattering due to quantum critical fluctuations: Perturbational approach. *J. Phys. Soc. Jpn* **71,** 867 (2002).
15. Kadowaki, K. & Woods, S. B. Universal relationship of the resistivity and specific heat in heavy-fermion compounds. *Solid State Commun.* **58,** 507–509 (1986).
16. Park, T. *et al.* Isotropic quantum scattering and unconventional superconductivity. *Nature* **456,** 366–368 (2008).
17. Gegenwart, P., Si, Q. & Steglich, F. Quantum criticality in heavy-fermion metals. *Nat. Phys* **4,** 186–197 (2008).
18. Wölfle, P. & Abrahams, E. Quasiparticles beyond the Fermi liquid and heavy fermion criticality. *Phys. Rev. B* **84,** 041101(R) (2011).
19. Stockert, O. *et al.* Magnetically driven superconductivity in $CeCu_2Si_2$. *Nat. Phys* **7,** 119–124 (2011).
20. Sato, N. K. *et al.* Strong coupling between local moments and superconducting 'heavy' electrons in UPd_2Al_3. *Nature* **410,** 340–343 (2001).
21. Saxena, S. S. *et al.* Superconductivity on the border of itinerant-electron ferromagnetism in UGe_2. *Nature* **406,** 587–592 (2000).
22. Levy, F., Sheikin, I., Grenier, B. & Huxley, A. D. Magnetic field-induced superconductivity in the ferromagnet URhGe. *Science* **309,** 1343–1346 (2005).
23. Huy, N. T. *et al.* Superconductivity on the border of weak itinerant ferromagnetism in UCoGe. *Phys. Rev. Lett.* **99,** 067006 (2007).

24. Hashimoto, K. *et al.* A sharp peak of the zero-temperature penetration depth at optimal composition in $BaFe_2(As_{1-x}P_x)_2$. *Science* **336,** 1554–1557 (2012).
25. Pixley, J. H., Deng, L., Ingersent, K. & Si, Q. Pairing correlations near a Kondo-destruction quantum critical point. Preprint at http://arxiv.org/abs/1308.0839 (2013).
26. Eiling, A. & Schilling, J. S. Pressure and temperature dependence of electrical resistivity of Pb and Sn from 1-300 K and 0-10 GPa-use as continuous resistive pressure monitor accurate over wide temperature range; superconductivity under pressure in Pb, Sn and In. *J. Phys. F* **11,** 623 (1981).

Acknowledgements
Work at Sungkyunkwan University was supported by a NRF grant funded by the Ministry of Science, ICT and Future Planning (No. 2012R1A3A2048816). Work at Los Alamos was performed under the auspices of the US Department of Energy, Office of Science, Division of Materials Science and Engineering.

Author contributions
All authors discussed the results and commented on the manuscript. S.S., E.P. and F.R. performed the measurements. E.D.B. provided the samples; J.N.K. and J.-H.S. performed the theoretical calculations; and T.P. and J.D.T. wrote the manuscript with input from all authors.

Additional information
Supplementary Information accompanies this paper at http://www.nature.com/naturecommunications

Competing financial interests: The authors declare no competing financial interest.

Reprints and permission information is available online at http://npg.nature.com/reprintsandpermissions/

How to cite this article: Seo, S. *et al.* Controlling superconductivity by tunable quantum critical points. *Nat. Commun.* 6:6433 doi: 10.1038/ncomms7433 (2015).